Published in "Journal of Physics B: Atomic, Molecular and Optical Physics 39(14): 2939-2947, 2006"
which should be cited to refer to this work.

Study of resonances in formic acid by means of vibrational excitation by slow electrons

Michael Allan

Department of Chemistry, University of Fribourg, Switzerland

Abstract

Absolute differential elastic and vibrational excitation cross sections have been measured for formic acid at 135° from threshold to 5 eV. Most vibrationally inelastic cross sections have a narrow peak at threshold, followed by a broadband with a boomerang structure due to the known π^* shape resonance. The cross section for the excitation of the O–H stretch vibration behaves differently, it also peaks at threshold, but then drops only slowly, with narrow cusp structures, and only a very weak influence of the π^* shape resonance. The cusp structures are even more pronounced in the cross section for the excitation of the O–H stretch overtone. The elastic cross section rises steeply at low energies. The π^* shape resonance decays also by the ejection of very slow electrons, exciting a vibrational quasicontinuum at large energy losses.

1. Introduction

Electron-induced processes in formic acid are important as a prototype for various biological systems and have been invoked to play a role in astrobiology [1]. An early electron transmission work revealed a π^* shape resonance with a boomerang structure at 1.9 eV [2, 3]. Very interesting phenomena were recently discovered in electron-driven chemistry (dissociative electron attachment) of formic acid and its clusters [1, 4–7]. The $HCOO^-$ formate anion signal appeared at its energetic threshold at 1.25 eV [4] despite the fact that direct dissociation of the a'' π^* shape resonance into the a' products is symmetry forbidden in the C_s group. The mechanism of the dissociative electron attachment was studied theoretically and the absence of the dissociation barrier was explained by Rescigno *et al* [8]. High signal-to-noise ratio spectrum revealed narrow structures on the dissociative electron attachment band [4]. An early dissociative electron attachment spectrum was reported by Muftakhov *et al* [9]. Calculations of resonances were reported by Gianturco and Lucchese [10].

This work aims at obtaining complementary data on the resonant processes in formic acid by measuring the cross sections for vibrational excitation. They are recorded as a function of

the incident electron energy in the range 0.05–5 eV. The scattering angle of 135° is chosen to emphasize the resonant phenomena and reduce the amount of direct dipole excitation which peaks in the forward direction. Vibrational excitation competes with dissociative electron attachment and provides rich complementary information on resonances. In particular, shape resonances strongly enhance vibrational excitation [11]. The selectivity of exciting various normal modes provides information on the ways in which the geometry of the negative ion is different from that of the neutral target and thus on the nature of the resonances [12]. The complementary vibrational excitation and dissociative electron attachment results can provide a deeper understanding of the dissociative electron attachment process, as exemplified by the work on chlorobenzene [13]. Vibrational excitation is also a suitable tool to study vibrational Feshbach resonances [14].

2. Experiment

The measurements were performed using a spectrometer with hemispherical analysers [15, 16]. The energy resolution was about 14 meV in the energy-loss mode, corresponding to about 10 meV in the incident electron beam, at a beam current of around 250 pA. The energy of the incident beam was calibrated on the 19.365 eV [17] ^{2}S resonance in helium and is accurate to within ±10 meV. The analyser response function was determined by elastic scattering in helium. The sample was introduced through a 0.25 mm diameter effusive nozzle kept at 35 °C. Absolute values of the cross sections were determined by comparison with the theoretical helium elastic cross section [18], as described in [15]. The elastic cross sections are accurate within about ±20%, the inelastic cross sections within about ±25%.

The pressure was kept low in the present experiments, both to minimize the formation of dimers and to prevent attenuation of low-energy scattered electrons by double scattering, which is particularly important for formic acid because of the very large elastic scattering cross section at very low energies (see the discussion of the elastic cross section below). The equilibrium constant for dimer formation and its temperature dependence have been measured by Taylor and Bruton [19]. Their formula indicates the value $K = 5.4$ Torr at 35°, the nozzle temperature of the present experiment. This in turn indicates that the ratio $r = P_m/P_d$ of the monomer and dimer partial pressures is $r = 0.97$ at a total pressure $P_t = 0.25$ mbars, $r = 0.89$ at $P_t = 1$ mbar and $r = 0.79$ at $P_t = 2.5$ mbars. The present measurement of the absolute elastic cross section was carried out at 2 eV at a nozzle backing pressure of 0.17 mbars where the dimer partial pressure is calculated to be less than 3% of the total pressure. The majority of the spectra were recorded at a nozzle backing pressure of 1 mbar, but it was verified that the spectra are essentially independent of the pressure between 0.25 and 2.5 mbars.

The liquid formic acid sample was kept at 0 °C, and the vapour under these conditions is known to contain a high percentage of dimers. This vapour was dosed by a needle valve, and then carried to the nozzle by a 6.35 mm diameter, 1 m long stainless steel tube, kept at 25 °C. The pressure in this tube (the nozzle backing pressure) could be measured with a capacitance manometer. The residence time in this tube gave ample time for the dimers to dissociate and reach their equilibrium partial pressure, since the chemical relaxation times under comparable conditions were found to be of the order of 10 μs [20]. To test whether the equilibrium partial pressures were really reached during the transit in the 1 m long inlet tube, a section of it was heated to about 100 °C for some time (to accelerate the dissociation) and it was verified that the spectra did not change.

These considerations indicate that the present results refer to the monomer, with dimer contributions below the error limit of the data. This statement is made under the plausible assumption that the elastic cross section of the dimer is not dramatically larger than that of

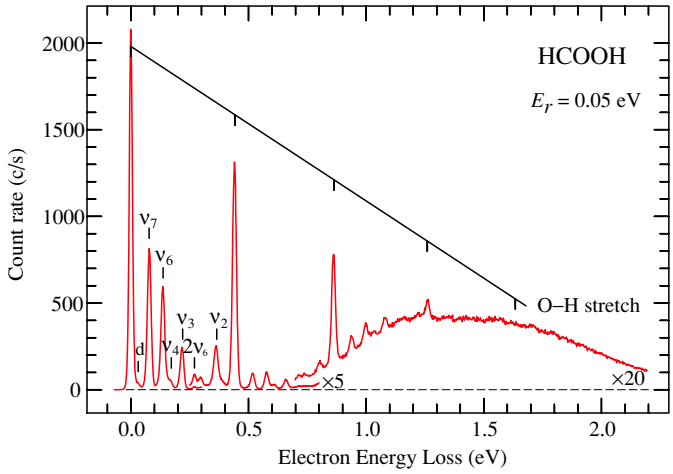

Figure 1. Near-threshold electron energy-loss spectrum recorded at a nozzle backing pressure of 1 mbar. The letter d denotes the wagging vibration of the dimer at 29 meV [21].

Table 1. Vibrational energies of formic acid [22].

Vibration	Sym. species	Type	Energy (meV)
ν_1	a′	O–H stretch	443
ν_2	a′	C–H stretch	365
ν_3	a′	C=O stretch	220
ν_4	a′	C–H bend	172
ν_5	a′	O–H bend	152
ν_6	a′	C–O stretch	137
ν_7	a′	O–C–O deformation	78
ν_8	a″	C–H bend	128
ν_9	a″	Torsion	79

the monomer at 2 eV. It should be noted that the situation is different in this respect for the dissociative electron attachment, where the dimer cross sections appear to exceed the monomer cross sections by orders of magnitude, yielding strong signals even with modest partial pressures of dimer [1].

3. Results and discussion

Figure 1 shows an electron energy-loss spectrum recorded by varying the incident electron energy and collecting slow scattered electrons with a residual energy of 50 meV. It shows which vibrational levels are excited very near threshold. A summary of the normal modes is given in table 1. The relative peak heights below an energy loss of about 0.15 eV are only qualitative—the efficiency of the instrument decreases at very low incident energies due to gradual loss of the incident electron beam, and the spectrum in figure 1 thus shows the elastic peak, and to a lesser degree the peak at $\Delta E = 79$ meV, too low. The spectrum in figure 1 reveals that many vibrations are excited at threshold, but that the O–H stretch is particularly active, the excitation of up to three quanta of this vibration is clearly visible. Apart from the ‘specific’ excitation of low quanta of discrete vibrational levels, ‘unspecific’

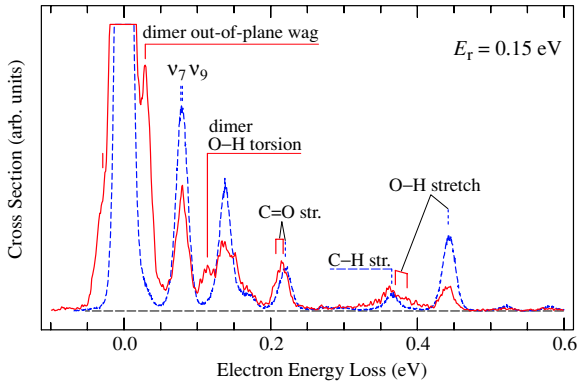

Figure 2. Electron energy-loss spectra recorded at backing pressures of 1 mbar (250 μm nozzle, dashed line) and about 60 mbars (30 μm nozzle, continuous line). Selected vibrations are marked by dashed (monomer) or solid (dimer) vertical bars.

excitation of a vibrational quasi-continuum through the a$''$ π^* shape resonance is observed as an underlying structureless band in the 0.7–2.2 eV energy loss range. This phenomenon is common in polyatomic molecules [23–26]. It has been studied theoretically by Gauyacq [27]. It is phenomenologically related to, and could have a similar origin as, the superinelastic electron transfer observed by Lu *et al* [28], where electrons attach to N_2 molecules adsorbed on a thin layer of frozen H_2O to form the $^2\Pi_g$ resonance, and then are transferred, with high probability, to unrelaxed traps in the water layer, depositing the energy released in the process in vibrational motion.

One feature in the spectrum in figure 1 can be identified as belonging to the dimer—the shoulder at 29 meV can be assigned to the dimer out-of-plane wagging vibration (no. 20 in [21]), with possible contributions of the nearby in-plane rock vibrations (nos. 19 and 21 in [21]). Its low intensity is consistent with the conclusion reached in the experimental section that the dimer partial pressure is low in the present experiment. It is also in line with the early electron energy-loss spectrum [2] which indicated that higher pressure conditions were required to yield discernable dimer vibrational peaks.

To further verify this critical assumption, an energy-loss spectrum was recorded at higher pressure, by taking formic acid vapour at its equilibrium pressure at room temperature (about 60 mbars), where a majority of the particles are dimers, and expanding it directly into the collision region through a 30 μm nozzle. The low and high pressure spectra are compared in figure 2. The weak shoulder at $\Delta E = 29$ meV in the low pressure spectrum becomes the dominant inelastic peak in the high pressure spectrum, confirming the low dimer concentration at low backing pressures. Several other dimer vibrations can be discerned in the high pressure spectrum. The O–H torsion vibration (no. 15 in [21]) is visible at 114 meV. The C=O stretch vibration of the monomer is shifted to lower energy and becomes broader, reflecting the splitting into a doublet in the dimer. The O–H stretch vibration is split and dramatically shifted to lower energies in the dimer. The higher of the two O–H stretch vibrations of the dimer can be clearly discerned at 386 meV in figure 2.

Electron energy-loss spectrum recorded at a constant incident energy corresponding to the π^* shape resonance is shown in figure 3. The spectrum is corrected for the analyser response function. Surprisingly, it is not very different from the threshold spectrum in the energy range of the 'specific' vibrational excitation. The π^* resonance would be expected to excite the C=O stretch vibration ν_3, the C–O stretch vibration ν_6 and the O–C–O bending

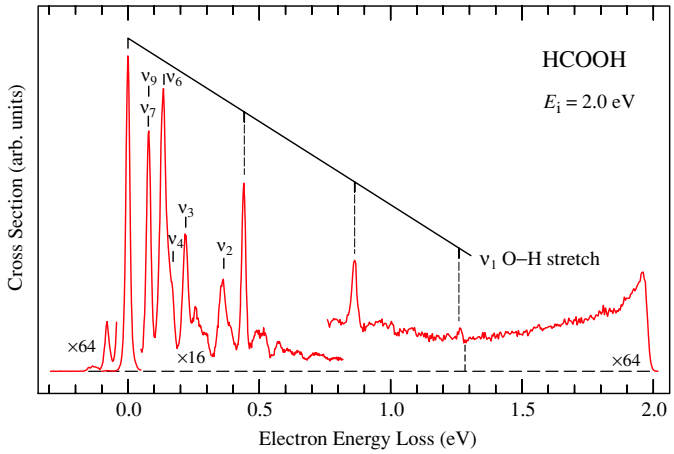

Figure 3. Electron energy-loss spectrum recorded at a constant incident energy situated within the π^* shape resonance. The nozzle backing pressure was 1 mbar. The dashed vertical line below the spectrum at 1.28 eV indicates where the division between the specific and the unspecific vibrational excitation has been taken for the purpose of determining the absolute cross sections of the two processes.

Table 2. Absolute differential cross sections at 2 eV and $\theta = 135^\circ$, in Å^2 sr^{-1} (1 Å^2 = 10^4 pm^2).

Process	$\partial\sigma/\partial\Omega$
Elastic	1.5
All inelastic processes	0.77
All inelastic processes up to $\Delta E = 1.28$ eV	0.65
All inelastic processes above $\Delta E = 1.28$ eV	0.12
Total (sum of elastic and inelastic)	2.27

vibration ν_7 by virtue of the bonding and antibonding properties of the temporarily occupied π^* orbital, and this expectation is confirmed by the spectrum. Excitation of three quanta of the O–H stretch vibration is observed, similar to the threshold spectrum, but it will be shown below that this excitation is not due to the π^* resonance. The spectrum provides a deeper insight into the nature of the unspecific excitation of the vibrational quasicontinuum—it is seen to peak at zero energy of the departing electron, as already observed earlier for other molecules [23–26]. At an intermediate range of energy losses both mechanisms are operative—specific vibrations are excited, superimposed on a vibrational quasicontinuum.

The areas under the inelastic peaks and the continuous signal in figure 1, together with the separately measured elastic cross section at 2 eV, were used to determine absolute differential inelastic cross sections at 2 eV and 135°. The areas under the individual narrow peaks in the specific vibrational excitation region were used to normalize the excitation functions, described below, to absolute values. The sum of the cross sections for all inelastic processes (both specific and unspecific vibrational excitations) has been obtained by integrating under the entire inelastic range of the spectrum, for energy losses between 0.05 and 2.0 eV, with the result given in table 2. The sum of all inelastic cross sections is seen to be quite large, about one half of the elastic cross section, making the total cross section 1.5 times larger than the elastic cross section at 2 eV and 135°.

It would be interesting to compare the relative importance of the specific and unspecific excitation cross sections. The two processes overlap and there is no unique criterion as to

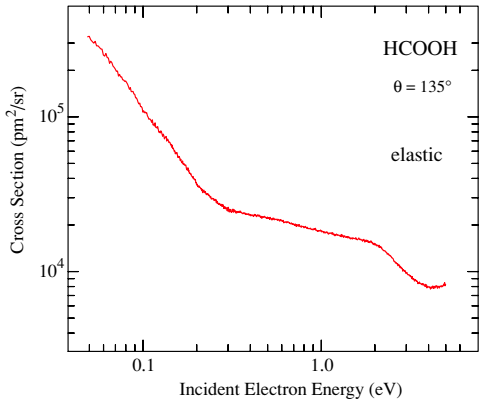

Figure 4. Elastic cross section.

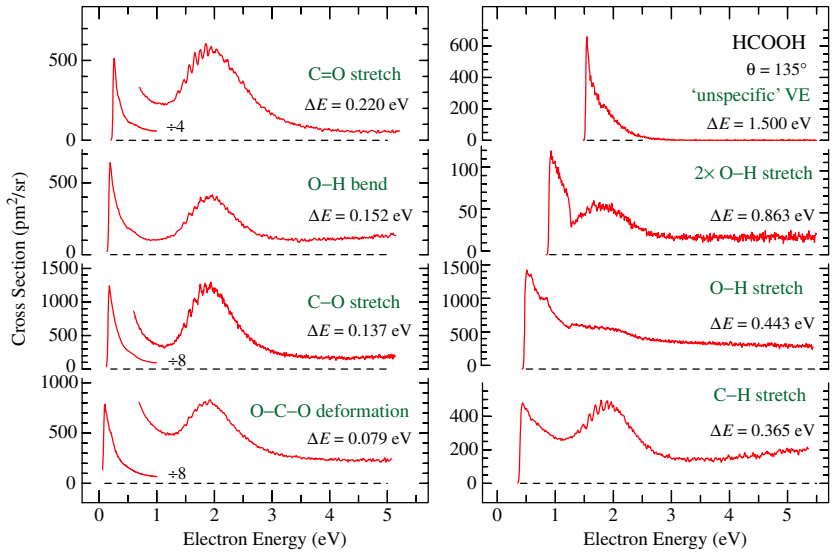

Figure 5. Cross sections for vibrational excitation.

where exactly they should be divided, but a useful qualitative indication is obtained when the division is drawn at the energy loss $\Delta E = 1.28$ eV, the minimum in the distribution of scattered electrons in figure 3. The results are also given in table 2. The specific vibrational excitation is found to be more intense by a factor of about 5. The unspecific vibrational excitation has been found to become more important with increasing molecular size [23, 25, 26].

Figure 4 shows the elastic cross section recorded as a function of electron energy. It rises to very large values at low energy, as expected because of the sizeable dipole moment of formic acid. The *trans* isomer, more stable than the *cis* isomer by 0.17 eV and predominant under the present conditions, has a dipole moment of 1.4 D ([29] and references therein). The π^* shape resonance causes a weak structure in the elastic cross section around 2 eV.

Selected vibrationally inelastic cross sections are shown in figure 5. In some cases there are ambiguities in the assignment of the vibrations, in particular ν_7 and ν_9 are nearly

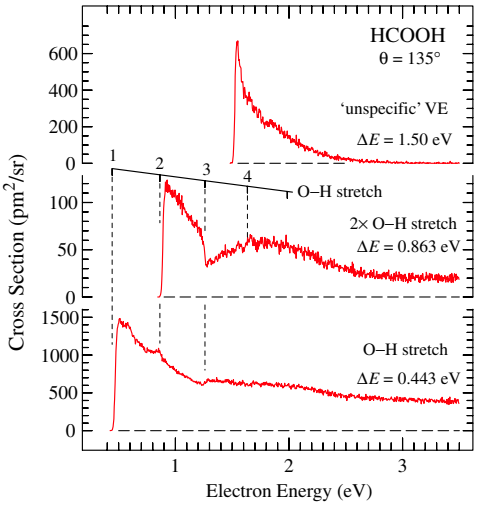

Figure 6. Detailed view of cross sections for vibrational excitation.

degenerate and the excitation function recorded with the energy loss $\Delta E = 79$ meV is the sum of the cross sections for the excitation of both vibrations. The nodal properties of the π^* orbital—it is bonding with respect to the O–O distance—indicate that the O–C–O angle becomes substantially smaller in the anion and explain the excitation of the O–C–O deformation vibration ν_7 in the π^* energy range. Measurement of the singly deuterated formic acid HCOOD indicated that both ν_7 and ν_9 are excited.

Several of the cross sections have very similar shapes—a narrow threshold peak followed by a broader band around 1.9 eV, due to the π^* shape resonance, with a boomerang structure already known from the early electron transmission study [2]. A notable exception is the cross section for the excitation of the O–H stretch vibration which also peaks at threshold but then decreases much slower than the remaining cross sections. This reveals an excitation mechanism other than the usual threshold peaks and other than the π^* shape resonance. It could be related to a O–H σ^* shape resonance, which is expected to lie above the π^* shape resonance [8], but to be very broad, so that it could affect vibrational excitation even below its nominal energy.

The O–H stretch excitation cross section further exhibits structures at the thresholds for the excitation of the higher O–H stretch quanta. The structures are more visible in the detailed view in figure 6. They become deeper in the cross section for the excitation of the O–H stretch overtone, in line with similar observations made in other molecules, for example in HF [30, 31] and CO_2 [32]. Structures of this type can be either cusps at vibrational thresholds, or vibrational Feshbach resonances [14]. A clear distinction is provided when the energy of the structure observed in the cross section is clearly below the vibrational threshold as for example in HF [30, 31]. In the present case the structures are not situated clearly below the vibrational thresholds and the question cannot, unfortunately, be clearly answered. They could be cusps, or vibrational Feshbach resonances situated below the threshold by an energy difference too small to be resolved in the present experiment.

The general shape of the present O–H stretch cross sections and the fact that they are excited even in higher overtones resemble the results in hydrogen halides [31, 33, 34], and bear out the similarities in electron scattering brought by the presence of an acidic hydrogen in a molecule. This similarity appears to extend even to dissociative electron attachment, where

a signal drop of the conjugate base $HCOO^-$ has been observed at 1.63 eV [4], the threshold for exciting four quanta of the O–H stretch vibration ν_1, analogous to the steps at vibrational thresholds reported for halogen halides [33, 35–37].

Figures 5 and 6 also show the cross section for the excitation of the vibrational quasicontinuum at an energy-loss $\Delta E = 1.5$ eV. Since the final state is not discrete in this case, the absolute value is given for a slice in the energy-loss spectrum with a width of $\Delta\Delta E = 0.10$ eV, that is, between $\Delta E = 1.45$ eV and $\Delta E = 1.55$ eV. It also has a weak cusp at the energy of one O–H stretch vibrational quantum above the onset.

4. Conclusions

The elastic cross section is very large at low energies and has a hump around 2 eV, due to the π^* shape resonance. The π^* shape resonance causes strong vibrational excitation; the vibrationally inelastic cross section summed over all vibrational levels amounts to 50% of the elastic cross section at 2 eV. There are two regimes of vibrational excitation in the π^* resonance region—the 'specific' vibrational excitation where specific vibrational modes are selectively excited up to an energy loss of about 1.2 eV, and the 'unspecific' vibrational excitation where a vibrational quasi-continuum is excited without selection with respect to the vibrational mode, peaking at zero energy of the scattered electrons. The prominent vibrational modes in the 'specific' excitation regime are those expected from the nodal properties of the temporarily occupied orbital: the C=O and C–O stretch modes ν_3 and ν_6, as well as the O–C–O bending mode ν_7. The vibrational cross sections recorded as a function of electron energy generally have a threshold peak and the π^* resonance band around 1.9 eV, with boomerang structure already known from early electron transmission experiments. The cross section for the excitation of the O–H stretch excitation ν_1 and its overtones have a different shape, also peaking at threshold but falling off much more slowly than the customary threshold peaks. Superimposed on this broadband are narrow structures, more pronounced in the overtone excitation, which could be cusps at vibrational thresholds or vibrational Feshbach resonances. Many analogies between the O–H stretch excitation in formic acid and vibrational excitation in hydrogen halides indicate general similarities in the physics of electron scattering in acids.

Acknowledgment

This research is part of project no. 200020-105226/1 of the Swiss National Science Foundation.

Note added in proof. Absolute differential elastic cross-sections for electron scattering from formic acid at incident electron energies from 1.8 to 50 eV were measured by Vizcaino *et al* [38] and their work appeared while this paper was in the publication process.

References

[1] Martin I, Skalický T, Langer J, Abdoul-Carime H, Karwasz G, Illenberger E, Stanob M and Matejcik S 2005 *Phys. Chem. Chem. Phys.* **7** 2212
[2] Tronc M, Allan M and Edard F 1987 *Electronic and Atomic Collisions: Abstracts of Contributed Papers of the XVth ICPEAC (Brighton, England)* ed J Geddes, H B Gilbody, A E Kingston, C J Latimer and H J R Walters (Amsterdam: North Holland) p 335
[3] Aflatooni A, Hitt B, Gallup G A and Burrow P D 2001 *J. Chem. Phys.* **115** 6489
[4] Pelc A, Sailer W, Scheier P, Mason N J, Illenberger E and Märk T D 2003 *Vacuum* **70** 429
[5] Sedlacko T, Balog R, Lafosse A, Stano M, Matejcik S, Azria R and Illenberger E 2005 *Phys. Chem. Chem. Phys.* **7** 1277
[6] Gianturco F A, Lucchese R R, Langer J, Martin I, Stano M, Karwasz G and Illenberger E 2005 *Eur. Phys. J.* D **35** 417

[7] Prabhudesai V S, Nandi D, Kelkar A H, Parajuli R and Krishnakumar E 2005 *Chem. Phys. Lett.* **405** 172
[8] Rescigno T N, Trevisan C S and Orel A E 2006 *Phys. Rev. Lett.* **96** 213201
[9] Muftakhov M V, Vasil'ev Y V and Mazunov V A 1999 *Rapid Commun. Mass Spectrom.* **13** 1104
[10] Gianturco F A and Lucchese R R 2004 *New J. Phys.* **6** 66
[11] Schulz G J 1973 *Rev. Mod. Phys.* **45** 423
[12] Walker I C, Stamatovic A and Wong S F 1978 *J. Chem. Phys.* **69** 5532
[13] Skalický T, Chollet C, Pasquier N and Allan M 2002 *Phys. Chem. Chem. Phys.* **4** 3583
[14] Hotop H, Ruf M-W, Allan M and Fabrikant I I 2003 *Adv. At. Mol. Phys.* **49** 85
[15] Allan M 2005 *J. Phys. B: At. Mol. Opt. Phys.* **38** 3655
[16] Allan M 1995 *J. Phys. B: At. Mol. Opt. Phys.* **28** 5163
[17] Gopalan A, Bömmels J, Götte S, Landwehr A, Franz K, Ruf M W, Hotop H and Bartschat K 2003 *Eur. Phys. J.* D **22** 17
[18] Nesbet R K 1979 *Phys. Rev.* A **20** 58
[19] Taylor M D and Bruton J 1952 *J. Am. Chem. Soc.* **74** 4151
[20] Winkler A, Mehl J B and Hess P 1994 *J. Chem. Phys.* **100** 2717
[21] Florio G M, Zwier T S, Myshakin E M, Jordan K D and Sibert E L III 2003 *J. Chem. Phys.* **118** 1735
[22] Shimanouchi T 1972 *Tables of Molecular Vibrational Frequencies, Consolidated* vol I (Washington, DC: National Bureau of Standards) pp 1–160
[23] Dressler R A and Allan M 1985 *Chem. Phys. Lett.* **118** 93
[24] Allan M 1984 *Chem. Phys.* **84** 311
[25] Allan M 1987 *Int. J. Quant. Chem.* **31** 161
[26] Allan M 1989 *J. Electron Spectrosc. Relat. Phenom.* **48** 219
[27] Gauyacq J-P 1990 *J. Phys. B: At. Mol. Opt. Phys.* **23** 3041
[28] Lu Q-B, Bass A D and Sanche L 2002 *Phys. Rev. Lett.* **88** 147601
[29] Brinkmann N R, Tschumper G S, Yan G and Schaefer H F III 2003 *J. Phys. C: Solid State Phys.* A **107** 10208
[30] Knoth G, Gote M, Rädle M, Jung K and Ehrhardt H 1989 *Phys. Rev. Lett.* **62** 1735
[31] Čížek M, Horáček J, Allan M, Fabrikant I I and Domcke W 2003 *J. Phys. B: At. Mol. Opt. Phys.* **36** 2837
[32] Allan M 2002 *J. Phys. B: At. Mol. Opt. Phys.* **35** L387
[33] Čížek M, Horáček J, Allan M, Sergenton A-C, Popović D, Domcke W, Leininger T and Gadea F X 2001 *Phys. Rev.* A **63** 062710
[34] Čížek M, Horáček J, Allan M and Domcke W 2002 *Czech. J. Phys.* **52** 1057
[35] Ziesel J P, Nenenr I and Schulz G J 1975 *J. Chem. Phys.* **63** 1943
[36] Abouaf R and Teillet-Billy D 1977 *J. Phys. B: At. Mol. Phys.* **10** 2261
[37] Abouaf R and Teillet-Billy D 1980 *Chem. Phys. Lett.* **73** 106
[38] Vizcaino V, Jelisavcic M, Sullivan J P and Buckman S J 2006 *New J. Phys.* **8** 85